Rev. Adv. Mater. Sci. 57 (2018) 1-10

A MODEL OF ENHANCED STRAIN RATE SENSITIVITY IN NANOCRYSTALLINE AND ULTRAFINE-GRAINED METALS

A.G. Sheinerman[1,2,3] and S.V. Bobylev[1,2]

[1]Institute of Problems of Mechanical Engineering, Russian Academy of Sciences, St. Petersburg 199178, Russia
[2]Peter the Great St. Petersburg Polytechnic University, St. Petersburg 195251, Russia
[3]Saint Petersburg State University, 7/9 Universitetskaya nab., St. Petersburg 199034, Russia

Received: April 30, 2018

Abstract. A model is suggested that describes enhanced strain rate sensitivity of nanocrystalline and ultrafine-grained metals. Within the model, plastic deformation of such metals incorporates dislocation transmission across grain boundaries (GBs) in the stress fields of dislocation pileups, the emission of individual dislocations from GBs as well as GB sliding accommodated by GB dislocation climb and/or Coble creep. The model predicts a strong increase in the strain rate sensitivity and a decrease in the activation volume with decreasing grain size, in accord with experimental data. We also considered the effect of GB sliding and Coble creep on the anomalous dependence of the activation volume on temperature observed in nanocrystalline Ni. It is demonstrated that although an account for GB sliding and Coble creep leads to the appearance of cusps in the temperature dependence of the activation volume, these mechanisms alone cannot be responsible for the observed anomalous dependence of the activation volume on temperature.

1. INTRODUCTION

Due to their superior mechanical properties (first of all, ultrahigh strength), ultrafine-grained and nanocrystalline solids attract tremendous attention [1-7]. The excellent mechanical properties of ultrafine-grained and nanocrystalline solids are strongly related to their enhanced strain rate sensitivity [7-12]. It is known [9,10,13,14] that even in the absence of the diffusion-controlled deformation mechanisms, such as grain boundary sliding accommodated by dislocation climb [15] or GB diffusion (Coble) creep [16], strain rate sensitivity of nanocrystalline metals can increase by more than order of magnitude as compared to that of coarse-grained or single-crystalline metals.

In general, two parameters generally describe the relation between the flow (or yield) stress and strain rate. In the case where the solid is under a uniaxial uniform load σ, the first one, strain rate sensitivity m, is defined as $m = \partial \ln\sigma / \partial \ln \dot{\varepsilon}$. The second one, activation volume V, is defined as $V = \sqrt{3}kT \cdot (\partial \ln \dot{\varepsilon} / \partial \sigma)$, where k is the Boltzmann constant and T the absolute temperature. These two parameters, related as $V = \sqrt{3}kT/(m\sigma)$, describe the thermally activated mechanisms that contribute to plastic deformation of metals and alloys. As the flow stress σ increases with a decrease in grain size, at least for the grain size above 20-30 nm, and strain rate sensitivity m increases with decreasing grain size, the latter relation predicts that activation volume decreases at small grain sizes, and this is confirmed by numerous experimental data.

Up to date, several mechanisms responsible for an increase in room temperature strain rate sensitivity (and the corresponding decrease in the activation volume) of ultrafine-grained and nanocrystalline

Corresponding author: A.G. Sheinerman, e-mail: asheinerman@gmail.com

metals have been suggested. Prasad and Armstrong [17] suggested that strain rate sensitivity is controlled by the thermally activated process of dislocation transmission across grain boundaries in the stress field of a dislocation pileup. They obtained the following relation between the inverse of the activation volume, V^{-1}, and the inverse square root of the grain size, $d^{-1/2}$ [17-21]:

$$V^{-1} = V_0^{-1} + \frac{k_{HP}}{2M\tau_c V_c} d^{-1/2}, \quad (1)$$

where $V_0 = MkT(\partial \ln \dot{\varepsilon} / \partial \sigma)$ is responsible for thermally activated deformation in grain interiors, $M \approx 3.06$ is the Taylor orientation factor [22], $k_{HP} = M(\tau_c G b)^{1/2}$ is the slope of the classical linear Hall–Petch dependence relating the yield stress σ with the inverse square root of the grain size $d^{-1/2}$, G is the shear modulus, b is the magnitude of the lattice dislocation Burgers vectors, τ_c is the critical shear stress at the grain boundary for the transmission of the head pileup dislocation to an adjacent grain, and $V_c = kT(\partial \ln \dot{\varepsilon} / \partial \sigma_c)$. Assuming that $\tau_c V_c$ does not depend on the grain size d, formula (1) predicts the linear dependence between V^{-1} and $d^{-1/2}$, which was confirmed by comparison with experimental data [21,23,24]. At the same time, since the parameters τ_c and V_c should depend on strain rate and temperature, formula (1) does not allow one to predict the dependence of the activation volume on the above two parameters.

Asaro and Suresh [8] examined plastic deformation in nanocrystalline metals realized via the generation and expansion of semi-circular partial glide dislocation loops at pre-existent grain boundary cracks and obtained the activation volume in the range $3–10b^3$, which is much smaller than the activation volume of course-grained metals.

Several authors [10,13,14,25,26] found that in nanocrystalline metals, activation volume can be a decreasing function of temperature, which is in contrast to coarse-grained metals, where activation volume typically increases with temperature [20,25]. This behavior was attributed [21,25,26] to the onset of diffusion-accommodated grain boundary sliding and/or Coble creep at elevated temperatures in nanocrystalline or ultrafine-grained solids.

Conrad [25] suggested the models describing the activation volume of metals with various grain sizes. He assumed that for course-grained metals, the strain rate controlling process is the dislocation intersection with forest dislocations, while in nanocrystalline metals with finest grains (below 10 nm) strain rate is controlled by diffusion accommodated grain boundary sliding or Coble creep. To explain a decrease of the activation volume with increasing temperature observed in some cases in ultrafine-grained and nanocrystalline metals, Conrad [25] assumed that in ultrafine-grained and nanocrystalline metals with the grain size above 10 nm plastic deformation is realized via thermally activated GB sliding that happens in the stress fields of lattice dislocation pileups. Although this model explained a decrease of the activation volume with increasing temperature, it completely neglected the process of thermally activated transmission of lattice dislocations across grain boundaries.

Kato [20,27] assumed that the strain rate controlling mechanism in nanocrystalline and ultrafine-grained metals is the depinning of the dislocations that move across a grain and have been pinned by grain boundary impurities or ledges. Under this assumption, Kato [20,27] obtained the anomalous dependence of the activation volume on temperature (a decrease in activation volume with an increase in temperature), in accord with experimental data for nanocrystalline Ni for the temperatures above 300K [10,21,25]. At the same time, Kato [20,27] obtained the anomalous temperature dependence for the physical activation volume, while the apparent activation volume, defined as $V = \sqrt{3}kT \cdot (\partial \ln \dot{\varepsilon} / \partial \sigma)$, demonstrated conventional temperature dependence (an increase in activation volume with an increase in temperature) in his model.

Thus, the model [17] where the dominant plastic deformation mechanism is dislocation transmission across grain boundaries calculates the grain size dependence of the activation volume but does not allow one to predict its dependence on the strain rate and temperature. Other models [25,27] ignore the process of the thermally activated dislocation transmission across grain boundaries, which should at least contribute to the strain rate sensitivity of ultrafine-grained and nanocrystalline metals. To fill this gap, here we suggest a model that examines the combined action of several deformation mechanisms in ultrafine-grained and nanocrystalline metals: 1) dislocation transmission across grain boundaries that occurs via the generation and expansion of dislocation loops at the head pileup dislocations, 2) generation of dislocations at pre-existent dislocations in grain boundaries and 3) grain boundary sliding accommodated by dislocation climb. We calculate the strain rate sensitivity and activation volume of ultrafine-grained and nanocrystalline metals as functions of grain size, strain rate and temperature and compare the results with available experimental data.

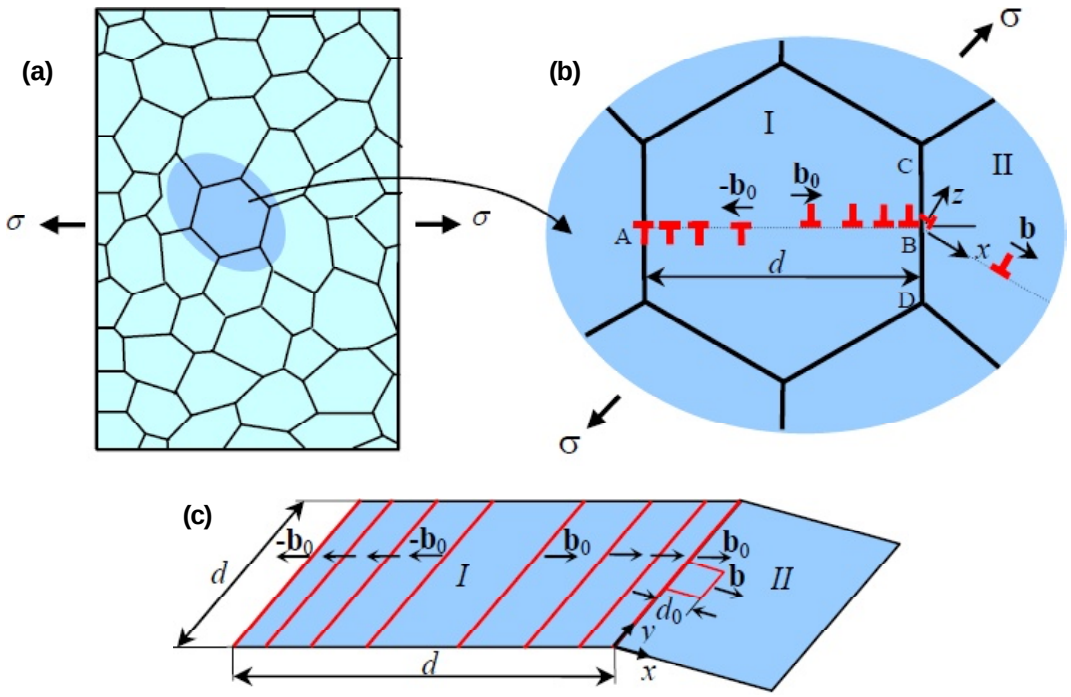

Fig. 1. Dislocation transmission across a grain boundary in polycrystalline metals. (a) Polycrystalline metallic specimen under uniaxial tensile loading. (b) Magnified fragment of figure (a) rotated by 45° highlights dislocation transmission across grain boundary CD in the stress field of the applied load σ and double dislocation pileup AB. (c) Dislocation transmission is illustrated in the plane normal to that shown in Figure (b), where the lines of the pileup dislocations and dislocation loop in grain II can be seen.

2. STRAIN RATE SENSITIVITY OF ULTRAFINE-GRAINED AND NANOCRYSTALLINE METALS. MODEL ASSUMPTIONS

Consider a metallic specimen under a uniaxial load and examine the micromechanisms of plastic deformation at the onset of plastic yielding. Within our model, we make the following assumptions:

1) The principal factors that can determine strain rate sensitivity in ultrafine-grained and nanocrystalline metals at the onset of plastic yielding are the dislocation transmission across grain boundaries (GBs), dislocation generation at GBs as well as GB sliding accommodated by GB dislocation climb and Coble creep.

2) Unless the grains are too small to provide the action of Frank–Read sources and accommodate dislocation pile-ups, at the onset of plastic deformation, the pile-ups form inside grains at Frank–Read sources, whose number density (number per unit volume) does not depend on grain size.

3) Dislocation transmission across GBs is realized via the formation of new glide dislocation loops at the head pileup dislocations located at GBs.

4) The expansion of subcritical dislocation loops is realized via thermal-fluctuation-assisted atomic jumps. Above the critical loop dimensions, the expansion of dislocation loops becomes energetically favored, and the loops expand through the glide of their segments.

5) At sufficiently small grain sizes, new glide dislocation loops can also nucleate at pre-existent non-equilibrium lattice dislocations at GBs, whose number per grain is proportional to the grain size.

3. STRAIN RATE SENSITIVITY AND ACTIVATION VOLUME OF NANOCRYSTALLINE AND ULTRAFINE-GRAINED METALS AT LOW HOMOLOGICAL TEMPERATURES

First, consider the case of low homological temperatures (T<(0.25-0.3)T_m, where T_m is the melting temperature), when GB sliding and Coble creep are not active. To calculate the strain rate sensitivity of ultrafine-grained and nanocrystalline metals, first, consider a metallic specimen under a uniform tensile load (Fig. 1a). Assume that a perfect glide dislocation loop nucleates in grain II at the head dislocation of a double dislocation pileup formed in grain I due to the action of a Frank–Read source (Figs.

1b and 1c). Let the length of the dislocation pileup be equal to the grain size d. Let the loop represent a square with a size d_0 and its sides be oriented along the x- and y-axes of the Cartesian coordinates system (x,y,z) (Fig. 1c). Let the Burgers vector of the pileup dislocations be denoted as $\mathbf{b}_0$ and the Burgers vector of the glide dislocation loop nucleating at the GB at the head pileup dislocation be designated as $\mathbf{b}$ (Figs. 1b and 1c). For simplicity, assume that the Burgers vector of the dislocation loop is directed along the x-axis (Fig. 1c). The magnitudes of the Burgers vectors $\mathbf{b}_0$ and $\mathbf{b}$ of perfect lattice dislocations and the dislocation loop are the same and specified as b.

We denote the energy associated with the formation of the critical dislocation loop (that is, the dislocation loop with the minimum possible area at which its further expansion in both directions becomes energetically favored) as ΔE_1 ($\Delta E_1>0$). Then the probability P_t of the generation of a critical glide dislocation loop at a specified site of the GB during the time t (small enough to guarantee that $P_t<<1$) can be written as $P_t = \nu_D t \exp[-\Delta E_1/(k_B T)]$, where ν_D is the Debye frequency of atomic jumps, k_B is the Boltzmann constant and T is the absolute temperature.

Let $J \approx d/b$ is the number of atoms at the head pileup dislocation at the GB. Then, accounting for the fact that critical loop size d_0 is much smaller than the length d of the head pileup dislocation, the number of sites (atoms) at which the loop can nucleate is approximately equal to J. As a result, the average number of the critical loops generated at the head pileup dislocations during time t is JP_t. The formation of a critical glide dislocation loop and its further expansion across a grain (which is assumed to be very fast compared to thermal-fluctuation-assisted nucleation of the critical loop) creates in this grain the average plastic strain sb/d, where s is the geometric factor of the order of unity. Then, assuming that the initial number of Frank–Read sources per unit volume is N and does not depend on grain size (although can differ from material to material), the average plastic strain ε_1 in the specimen due to multiple generation and expansion of dislocation loops at head pileup dislocations at GBs is $\varepsilon_1 = Nbd^2 sJP_t$, which yields

$$\varepsilon_1 = Nsd^3 \nu_D t \exp[-\Delta E_1 / (k_B T)]. \qquad (2)$$

Since $t = \varepsilon_1/\dot{\varepsilon}_1$, where $\dot{\varepsilon}_1$ is the plastic strain rate, formula (2) gives

$$\dot{\varepsilon}_1 = K_1 d^3 \exp[-\Delta E_1 / (k_B T)]. \qquad (3)$$

where $K_1 = Ns\nu_D$. Formula (3) is valid for small plastic strains, at the onset of plastic yielding, when the applied load σ equals the yield strength σ_y.

Let us denote the resolved shear stress, created in the xz-plane by the applied load σ and all the pileup dislocations apart from the head one, as $\tau = \tau_{xz}$. Then the energy ΔE_1 associated with the formation of an individual critical glide dislocation loop incorporates the proper energy of the dislocation loop, the energy of its interaction with the head pileup dislocation, and the opposite of the work of the resolved shear stress τ on its formation. The energy ΔE_1 is given by [28] and can be written as

$$\Delta E_1 = \beta D b^2 d_0 \ln\frac{\kappa d_0}{b} - \tau b d_0^2, \qquad (4)$$

where $D = G/[2\pi(1-\nu)]$, G is the shear modulus, ν is Poisson's ratio, β is the factor that depends on the angles between the Burgers vectors $\mathbf{b}_0$ and $\mathbf{b}$ of the head pileup dislocation and the glide dislocation loop, respectively, and κ is the factor of the order of unity that accounts for the energy of the dislocation loop core. For the critical dislocation loop, we have: $\partial\Delta E_1/\partial d_0 = 0$, which, in couple with formula (4), yields:

$$\frac{\ln x}{x} = A, \qquad (5)$$

where $x = \kappa e d_0/b$ and $A = 2\tau/(\beta D \kappa e)$. The solution to Eq. (5) gives the critical dislocation loop size, and this solution exists for $A \le 1/e$, that is, at $\tau \le \beta D\kappa/2$. (In the hypothetic case of extremely high stresses, where $\tau > \beta D\kappa/2$, ΔE_1 is always negative, and the energetic barrier for loop formation is absent, which can lead to extremely high strain rates.)

The solution to Eq. (5) for $A \le 1/e$ under the condition $\Delta E_1(A=0)>0$ has the form

$$x = -\frac{W_{-1}(-A)}{A}, \qquad (6)$$

where $W_{-1}(-A)$ is the Lambert-W function. From formulae (4)–(6) and the relation $e^{-W_{-1}(-A)} = -W_{-1}(-A)/A$, we obtain: $\Delta E_1 = (Db^3/\tilde{\kappa})f(A)$, where $\tilde{\kappa} = \kappa e/\beta$ and

$$f(A) = \frac{W_{-1}(-A)}{2A}(W_{-1}(-A) + 2). \qquad (7)$$

Now calculate the shear stress τ acting on the dislocation loop and created by the dislocation pileup (excluding the head dislocation) and the applied load σ. The stress τ at the head of the dislocation pileup can be presented [29] as

$$\tau = \frac{\alpha d(\sigma_y - \sigma_0)^2}{8Db}, \tag{8}$$

where α is the factor depending on the directions of the lines of the pileup dislocations and the Burgers vectors $\mathbf{b}_0$ and $\mathbf{b}$ with respect to the direction of the applied load, and σ_0 is the stress associated with the Peierls barrier to dislocation motion and the interactions among the forest dislocations inside coarse grains. (The stress σ_0 can be considered as the tensile yield strength of a coarse-grained solid with a large enough grain size.)

Formula (8) and the relation $A = 2\tau/(\beta D\kappa e)$ give: $A = P(\sigma_y - \sigma_0)^2 d/(D^2 b)$, where $P = \alpha/(4\beta\kappa e)$. The above expression for A in combination with the relation $\Delta E_1 = (Db^3/\tilde{\kappa})f(A)$ as well as formulae (3), (7), and (8) give the relation between the strain rate $\dot{\varepsilon}_1$ and the yield strength σ_y.

Now consider the case where, in addition to the generation at the head dislocations of dislocation pileups, glide dislocation loops nucleate at individual pre-existent non-equilibrium dislocations at GBs, whose number per grain is proportional to grain size. (Since the length of the non-equilibrium dislocations at GBs is proportional to the grain size, the latter assumption implies that the density of non-equilibrium dislocations at GBs (defined as the total length of dislocation lines per unit volume) does not depend on grain size.) In this case, the plastic strain rate $\dot{\varepsilon}_2$ associated with plastic deformation due to the formation and expansion of dislocation loops generated at individual nonequilibrium dislocations in GBs can be written similar to formula (3) for $\dot{\varepsilon}_1$ as

$$\dot{\varepsilon}_2 = K_2 d \exp[-\Delta E_2 / (k_B T)], \tag{9}$$

where K_2 is a factor that does not depend on grain size d and ΔE_2 is the energy associated with the formation of a critical glide dislocation loop at an individual lattice dislocation in a GB. In this case, the average shear stress $\tau' = \tau'_{xz}$ acting on the dislocation loop (Fig. 1c) can be written as $\tau' = \sigma_y/M$, where M is the Taylor factor, as above. From this, similar to the expression for $\dot{\varepsilon}_1$ (defined by formula (3) and the relation $\Delta E_1 = (Db^3/\tilde{\kappa})f(A)$), we have:

$$\dot{\varepsilon}_2 = K_2 d \exp\left[-\frac{Db^3}{\tilde{\kappa}k_B T} f\left(\frac{P_1\sigma_y}{D}\right)\right], \tag{10}$$

where $P_1 = 8P/(\alpha M)$ is the material parameter of the order of unity.

The total plastic strain rate $\dot{\varepsilon}$ is the sum of $\dot{\varepsilon}_1$ and $\dot{\varepsilon}_2$:

$$\dot{\varepsilon} = \dot{\varepsilon}_1 + \dot{\varepsilon}_2 = K_1 d^3 \exp\left[-\frac{Db^3}{\tilde{\kappa}k_B T} f\left(\frac{P(\sigma_y - \sigma_0)^2 d}{D^2 b}\right)\right] + K_2 d \exp\left[-\frac{Db^3}{\tilde{\kappa}k_B T} f\left(\frac{P_1\sigma_y}{D}\right)\right]. \tag{11}$$

The numerical solution to Eq. (11) for σ_y allows one to plot the dependences of the yield strength σ_y on grain size d, for various values of $\dot{\varepsilon}$. Also, the strain rate sensitivity m at the onset of plastic yielding is derived from formula (11) and the definition $m = \dot{\varepsilon}/(\sigma_y \partial\dot{\varepsilon}/\partial\sigma_y)$ as

$$m = -\frac{\dot{\varepsilon}\tilde{\kappa}k_B T}{\sigma_y b^3 d K_1}\left\{\frac{2P(\sigma_y - \sigma_0)d^3}{Db}\frac{\partial f}{\partial A}\left(\frac{P(\sigma_y - \sigma_0)^2 d}{D^2 b}\right)\exp\left[-\frac{Db^3}{\tilde{\kappa}k_B T} f\left(\frac{P(\sigma_y - \sigma_0)^2 d}{D^2 b}\right)\right] + \right.$$
$$\left.\frac{K_2}{K_1} P_1 \frac{\partial f}{\partial A}\left(\frac{P_1\sigma_y}{D}\right)\exp\left[-\frac{Db^3}{\tilde{\kappa}k_B T} f\left(\frac{P_1\sigma_y}{D}\right)\right]\right\}^{-1}. \tag{12}$$

Formula (12) and the numerical solution to Eq. (11) for σ_y enables one to plot the strain rate sensitivity m as a function of d and $\dot{\varepsilon}$.

Let us calculate the yield strength σ_y and strain rate sensitivity m for the case of Cu characterized by the following parameter values: G = 46 GPa, ν = 0.34, σ_0 = 25 MPa, b = 0.25 nm. We also put T = 300K, $\tilde{\kappa}$ = 150, P = 0.12, p_1 = 0.84, K_2/K_1 = 1 μm². The dependences of σ_y on $d^{-1/2}$ for Cu deformed at various values of the parameter $\dot{\varepsilon}$ are shown in Fig. 2. Fig. 2 demonstrates that for coarse-grained Cu, the dependence of σ_y on $d^{-1/2}$ is linear, that is, it strictly follows the Hall–Petch relation [30]. At the same time, in the

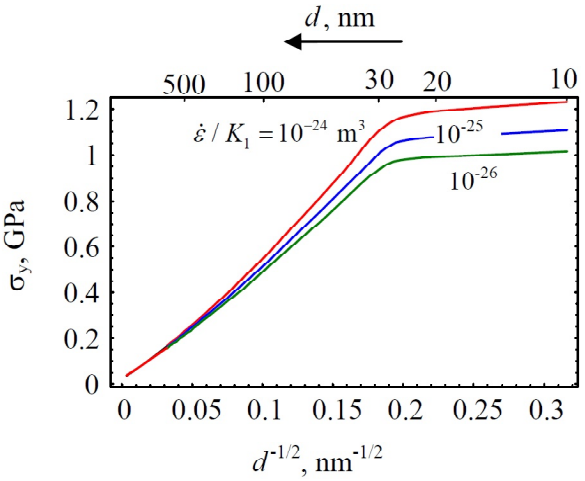

Fig. 2. The dependences of the yield strength σ_y for polycrystalline Cu on the inverse square root, $d^{-1/2}$, of grain size d, for various values of $\dot{\varepsilon}/K_1$.

submicrocrystalline and especially nanocrystalline range, the slope of the σ_y vs $d^{-1/2}$ curve increases, and the increase of the slope becomes more pronounced at higher strain rates. The large difference between the values of the yield strength at various strain rates in the nanocrystalline range points to a significant enhancement of the strain rate sensitivity at nanoscopic grain sizes. At the same time, at very small grain sizes (below 25 nm), when the dominant deformation mechanisms is dislocation emission from GBs, the slope of the dependence of σ_y on $d^{-1/2}$ strongly decreases.

The strain rate sensitivity m as a function of grain size d for Cu is plotted in Fig. 3, for various values of the parameter $\dot{\varepsilon}/K_1$. Fig. 3 demonstrates that m increases with decreasing grain size d and the enhancement of m is significant for ultrafine-grained and nanocrystalline metals. Fig. 3 also demonstrates that for nanocrystalline metals strain rate sensitivity strongly depends not only on grain size but also on strain rate. The calculated values of the strain rate sensitivity m for Cu agree well with experimental data [9,31-36] if plastic deformation proceeds via both dislocation transmission across GBs and dislocation generation at individual GBs, and the best agreement in the region of finest grains is achieved for the highest curve corresponding to a high strain rate.

Fig. 4 illustrates the dependences of the normalized inverse activation volume b^3/V of polycrystalline Cu on $d^{-1/2}$. Fig. 4 demonstrates that at grain sizes below several hundreds nanometers, b^3/V increases linearly with $d^{-1/2}$, in accord with the model of Prasad and Armstrong [17]. At higher grain sizes, however, the slope of the dependence of b^3/V on $d^{-1/2}$ increases with increasing $d^{-1/2}$. A change in the slope of the dependence of b^3/V on $d^{-1/2}$ arises in our model due to the dependence of the slope k_{HP} of the Hall–Petch dependence on the grain size, which is, in turn, associated with the grain size dependence of strain rate sensitivity. Fig. 4 also demonstrates that the activation volume also strongly depends on strain rate and can alter by a factor of two when the strain rate changes by two orders of magnitude. This means that the experimental data on the activation volume of ultrafine-grained and nanocrystalline metals should include strain rate as an important parameter, along with grain size, temperature and strain.

4. STRAIN RATE SENSITIVITY AND ACTIVATION VOLUME AT ELEVATED TEMPERATURES

Now consider the situation of ultrasmall grain sizes and/or elevated temperatures, where diffusion-as-

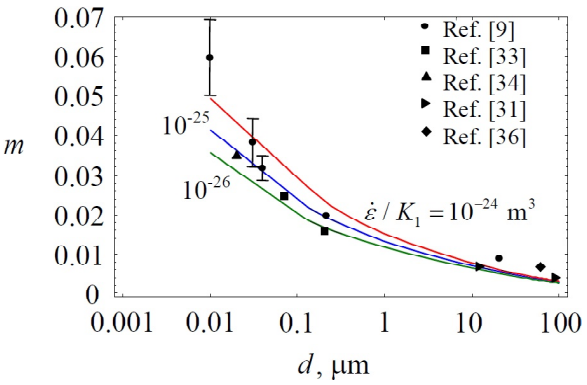

Fig. 3. Strain rate sensitivity m of polycrystalline Cu vs grain size d, for various values of $\dot{\varepsilon}/K_1$.

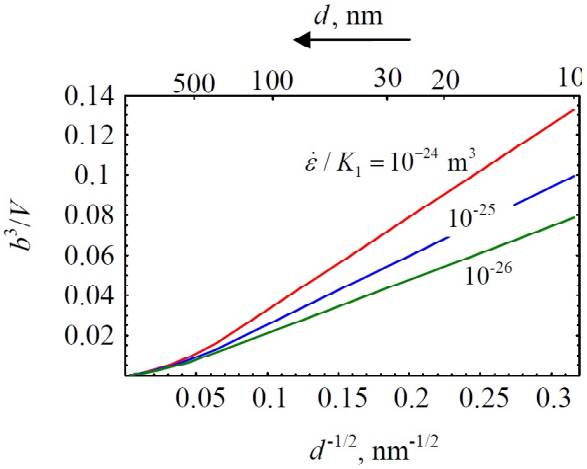

Fig. 4. Dependences of the normalized inverse activation volume b^3/V of polycrystalline Cu on the inverse square root, $d^{-1/2}$, of grain size d, for various values of $\dot{\varepsilon}/K_1$.

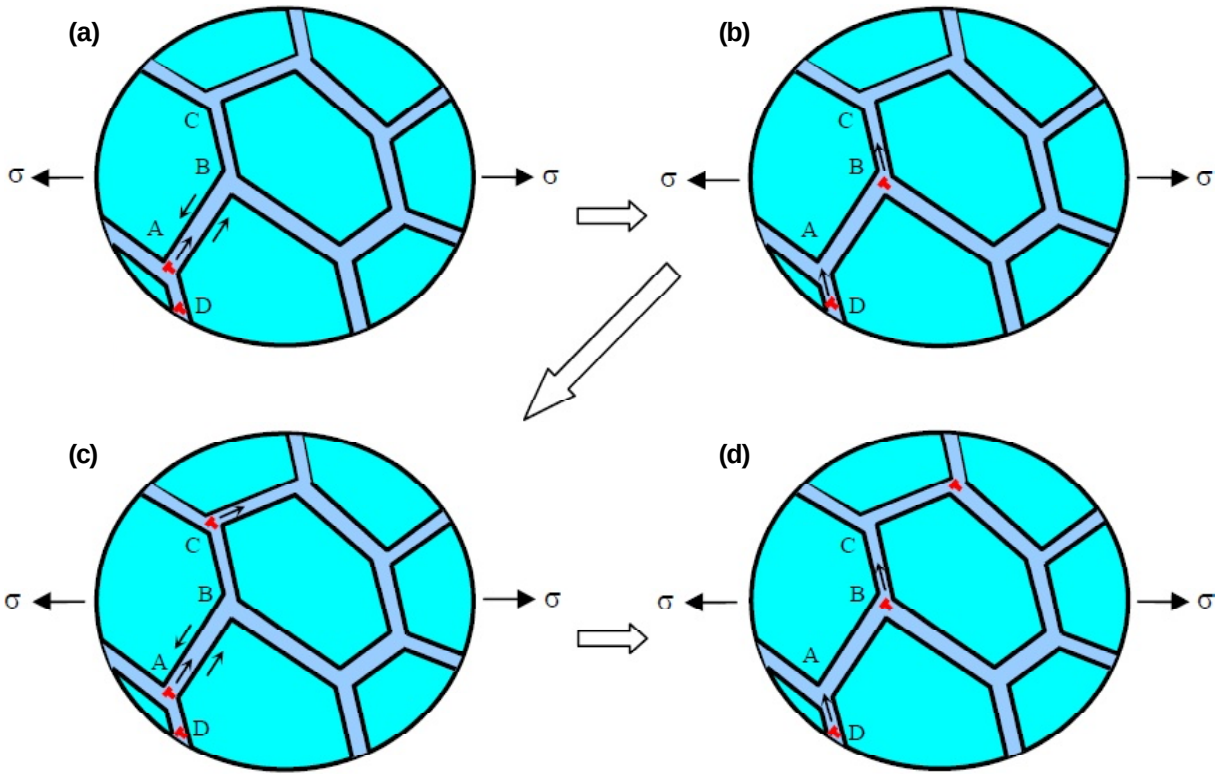

Fig. 5. Grain boundary sliding accommodated by grain boundary dislocation climb in a deformed metallic solid. (a) A fragment of a nanocrystalline or ultrafine-grained metallic solid under a uniform tensile stress σ. The slip of a grain boundary dislocation along grain boundary AB results in sliding over this boundary. (b) Grain boundary dislocation climbs from triple junction B over neighboring grain boundary BC. At the same time, new grain boundary dislocation comes to grain boundary AD. (c) Grain boundary dislocation at grain boundary AD reaches triple junction A and starts to slip along grain boundary AB, providing further sliding over this grain boundary. (d) Climb of grain boundary dislocations over grain boundaries BC and AD repeats.

sisted deformation mechanisms can be activated in metals. Assume that in this case, in addition to lattice dislocation motion, GB sliding accommodated by dislocation climb takes place in an ultrafine-grained or nanocrystalline metallic solid (Fig. 5). Within our model, GB sliding is carried by GB dislocations that slip over GBs from one triple junction to another under the action of the resolved shear stress (Figs. 5a and 5b). Next, these dislocations climb along neighboring GBs and move away from these triple junctions (Fig. 5c). The processes of GB sliding and dislocation climb repeat (Fig. 5d), resulting in macroscopic GB sliding.

To estimate the critical stress for the onset of GB sliding, assume that GB sliding is controlled by the possibility for dislocation climb. Then the rate ν_c of the dislocation climb can be written [37] as

$$\nu_c = \frac{D_{GB}}{h}\left[\exp\left(\frac{\sigma_{nn} b^3}{k_B T}\right) - 1\right], \qquad (13)$$

where D_{GB} is the GB self-diffusion coefficient, h is the screening length of the dislocation stress field, b is the perfect lattice dislocation Burgers vector, as above, σ_{nn} is the component of the stress field created by the applied load, and **n** is the normal to the GB along which the dislocation climbs.

The strain rate $\dot{\varepsilon}_{GBS}$ associated with GB sliding can be roughly estimated [15] as $\dot{\varepsilon}_{GBS} = b_{GB}\nu_c/(\sqrt{3}dh)$, where d is the grain size, and b_{GB} is the magnitude of the GB dislocation Burgers vector. In the case of uniaxial deformation, the applied load σ can be related to the stress σ_{nn} as $\sigma = \sigma_{nn}/M_1$, where M_1 is the factor of the order of unity. By assuming $h = d/\sqrt{3}$ and $\sigma = \sigma_y$, the latter relations combined with formula (13) yield:

$$\dot{\varepsilon}_{GBS} = \frac{\sqrt{3} D_{GB} b_{GB}}{d^3}\left[\exp\left(\frac{\sigma_y b^3}{M_1 k_B T}\right) - 1\right]. \qquad (14)$$

It should be noted that the character of the dependence of strain rate on the applied load, temperature and grain size is similar to that due to the Coble creep [16], so that as a first approximation, formula (14) can describe the action of both GB slid-

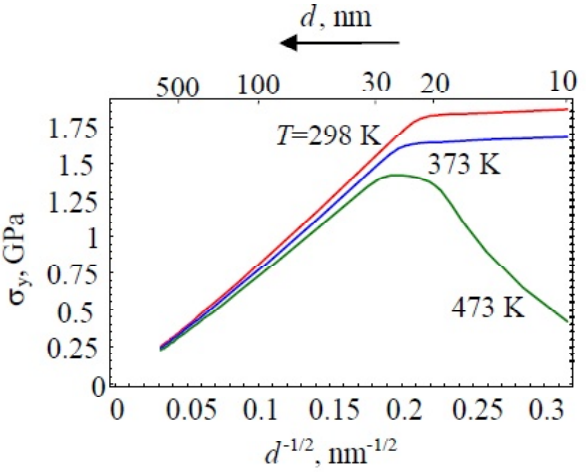

Fig. 6. The dependences of the yield strength σ_y for polycrystalline Ni on the inverse square root, $d^{-1/2}$, of grain size d, for various values of absolute temperature T.

ing accommodated by dislocation climb and Coble creep.

Now the total plastic strain rate $\dot{\varepsilon}_{tot}$ can be presented as the sum of $\dot{\varepsilon}$ (given by formula (11)) and $\dot{\varepsilon}_{GBS}$ (given by formula (14)): $\dot{\varepsilon}_{tot} = \dot{\varepsilon} + \dot{\varepsilon}_{GBS}$. The numerical solution for the latter equation for σ_y allows one to plot the dependences of the yield strength σ_y on grain size d, for various values of $\dot{\varepsilon}$. Let us calculate the yield strength σ_y for the case of Ni characterized by the following parameter values: $G = 76$ GPa, $\nu = 0.31$, $\sigma_0 = 30$ MPa, $b = 0.25$ nm. We also put $K_1 = 10^{23}$ s^{-1} m^{-3}, $M_1 = 1.5$, $b_{GB} = 0.1$ nm, $D_{GB} = D_{GB0}e^{-Q/(RT)}$ (where $R = 8.31$ J·mol^{-1}K^{-1} is the universal gas constant, D_{GB0} is the pre-exponential factor, and Q is the activation energy of GB self-diffusion of Ni), $\dot{\varepsilon}_{tot} = 10^{-4}$ s^{-1}, and $\tilde{\kappa} = 150$, $P = 0.12$, $P_1 = 0.84$, $K_2/K_1 = 1$ μm^2, as above. First, we assume that the values of D_{GB0} and Q for nanocrystalline Ni are equal to the values of the corresponding parameters of high-purity coarse-grained Ni [38] and set $D_{GB0} = 10^{-5}$ m^{2}s^{-1} and $Q = 123$ KJ/mol.

The dependences of σ_y on $d^{-1/2}$ for Ni deformed at various values of temperature T are shown in Fig. 6. Fig. 6 demonstrates that at the diffusion rate corresponding to that of coarse-grained Ni, GB sliding in nanocrystalline Ni starts at a temperature above 400K, leading to a decrease of the yield strength σ_y with a decrease in grain size d at sufficiently small grain sizes and high enough temperatures (see the lowest curve in Fig. 6). At these temperatures, yield strength as a function of grain size follows the inverse Hall–Petch dependence [39, 40].

Using the relation between the strain rate and yield strength (given by formulae (11) and (14) as

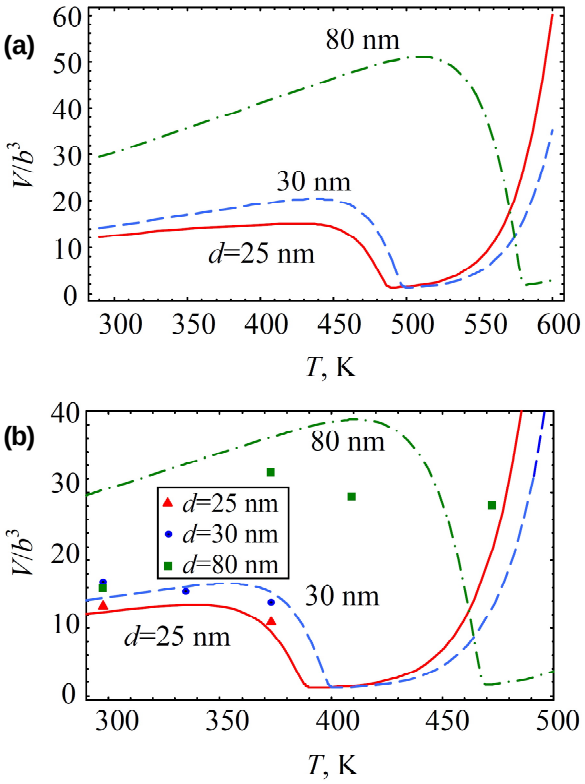

Fig. 7. Normalized activation volume of nanocrystalline Ni vs temperature, for various values of Ni grain size d. Figures (a) and (b) correspond to the two different values of the activation energy Q of grain boundary self-diffusion of nanocrystalline Ni: (a) $Q = 123$ kJ/mol and (b) $Q = 101$ kJ/mol. The experimental points shown in (b) are taken from [21] based on the strain rate sensitivity measurements of [13,14].

well as the equality $\dot{\varepsilon}_{tot} = \dot{\varepsilon} + \dot{\varepsilon}_{GBS}$), we have calculated the activation volume V in the examined case where GB sliding and/or Coble creep is active in the deformed Ni specimen in addition to lattice dislocation motion. Fig. 7a plots the normalized activation volume V/b^3 as a function of temperature T, for the parameter values specified above and three different values of grain size, $d = 25$, 30, and 80 nm. Fig. 7a demonstrates that the activation volume increases with temperature up to the temperatures of 420–500K, when GB sliding or Coble creep becomes active. The dependence of activation volume on temperature in Fig. 7a does not agree, however, with the experimental data [13,14,21] that demonstrate that in nanocrystalline Ni, activation volume can be a decreasing function of temperature at smaller temperatures. To verify whether the above effect (a decrease in activation volume with temperature at temperature above the room one) can be associated with GB sliding or Coble creep, we assumed that

the GB diffusion activation energy in nanocrystalline Ni can be smaller (and GB diffusion rate is, respectively, higher) than that of high-purity coarse-grained Ni and put Q = 101 KJ/mol for nanocrystalline Ni. The dependences of the normalized activation volume V/b^3 on temperature T for this value of the parameter Q are presented in Fig. 7b. For comparison, Fig. 7 also shows the experimental data on the temperature dependence of the activation volume in nanocrystalline Ni. The theoretical curves in Fig. 7b demonstrate that activation volume first increases, then abruptly decreases and then increases again with increasing temperature. The cusps in the dependences of the activation volume on temperature are associated with the action of GB sliding. Since the activation volume V can be written as $V = \sqrt{3}kT/(m\sigma_y)$, an abrupt decrease in the activation volume can be related to the abrupt increase in the strain rate sensitivity m, while its further increase with increasing temperature can be related, first, to a decrease in the yield stress σ_y and, second, to an increase in temperature T. Fig. 7b demonstrates that, when one selects a specific value of the GB diffusion activation energy, the theoretical curves can reasonably well fit the experimental data on the specimens with the grain sizes of 25 and 30 nm. However, they still cannot fit the experimental data for the specimen with the grain size of 80 nm. This means that in parallel with GB sliding, some other plastic deformation processes should be responsible for the observed anomalous temperature dependence of the activation volume (decrease in the activation volume with temperature) in nanocrystalline Ni, whose identification needs further investigations.

5. CONCLUSIONS

To summarize, we have suggested a model that describes enhanced strain rate sensitivity of ultrafine-grained and nanocrystalline metals. Within the model, the yield strength of such metals is controlled by lattice dislocation transmission across grain boundaries in the stress fields of dislocation pileups, the generation of lattice dislocations at grain boundaries at pre-existent individual lattice dislocations as well as GB sliding accommodated by GB dislocation climb and/or Coble creep. We calculated the yield strength and strain rate sensitivity of metals as functions of grain size and strain rate. The results for Cu demonstrate a considerable increase in the strain rate sensitivity and the corresponding decrease in the activation volume in the ultrafine-grained and especially nanocrystalline range even in the absence of GB sliding or Coble creep, and the calculated values of strain rate sensitivity agree well with experimental data. We also analyzed the effect of GB sliding on the activation volume of nanocrystalline Ni in the temperature interval of 300–500K. The analysis demonstrated that the anomalous temperature dependence of the activation volume (a decrease in the activation volume with an increase in temperature) observed in nanocrystalline Ni cannot be explained by the action of GB sliding or Coble creep, and the reasons for such anomalous behavior of the activation volume have yet to be identified.

ACNOWLEDGEMENTS

The work was supported by the Russian Ministry of Education and Science (task 16.3483.2017/PCh), Saint Petersburg State University via Lot 2017 Applied (Id:26130576) and, in part (for SVB), by the Council for grants of the President of Russian Federation (grant MD-3154.2017.1).

REFERENCES

[1] X. Sauvage, G. Wilde, S.V. Divinski, Z. Horita and R.Z. Valiev // *Mat. Sci. Eng. A* **540** (2012) 1.
[2] Y. Huang and T.G. Langdon // *Mater. Today* **16** (2013) 85.
[3] M. Kawasaki and T.G. Langdon // *J. Mater. Sci.* **51** (2016) 19.
[4] P. Kumar, M. Kawasaki and T.G. Langdon // *J. Mater. Sci.* **51** (2016) 7.
[5] A. Prakash, D. Weygand and E. Bitzek // *Int. J. Plasticity* **97** (2017) 107.
[6] V. Borovikov, M.I. Mendelev and A.H. King // *Int. J. Plasticity* **90** (2017) 146.
[7] I.A. Ovid'ko, R.Z. Valiev and Y.T. Zhu // *Prog. Mater. Sci.* **94** (2018) 462.
[8] R.J. Asaro and S. Suresh // *Acta Mater.* **53** (2005) 3369.
[9] J. Chen, L. Lu and K. Lu // *Scripta Mater.* **54** (2006) 1913.
[10] Y. Wang, A. Hamza and E. Ma // *Acta Mater.* **54** (2006) 2715.
[11] I.A. Ovid'ko and A.G. Sheinerman // *Acta Mater.* **58** (2010) 5286.
[12] I.A. Ovid'ko and A.G. Sheinerman // *Int. J. Plasticity* **96** (2017) 227.
[13] Y.J. Li, J. Mueller, H.W. Höppel, M. Göken and W. Blum // *Acta Mater.* **55** (2007) 5708.
[14] G. Mohanty, J.M. Wheeler, R. Raghavan, J. Wehrs, M. Hasegawa, S. Mischler,

L. Philippe and J. Michler // *Philos. Mag.* **95** (2015) 1878.
[15] T.G. Langdon // *Acta Metall. Mater.* **42** (1994) 2437.
[16] R.L. Coble // *J. Appl. Phys*. **34** (1963) 1679.
[17] Y.V.R.K. Prasad and R.W. Armstrong // *Philos. Mag.* **29** (1974) 1421.
[18] P. Rodriguez // *Metall. Mater. Trans. A* **35** (2004) 2697.
[19] R.W. Armstrong and P. Rodriguez // *Philos. Mag.* **86** (2006) 5787.
[20] M. Kato // *Mater. Trans.* **55** (2014) 19.
[21] R.W. Armstrong and N. Balasubramanian // *AIP Advances* **7** (2017) 085010.
[22] G.I. Taylor // *Journal of the Institute of Metals* **62** (1938) 307.
[23] R.W. Armstrong // *Philos. Mag.* **96** (2016) 3097.
[24] R. Armstrong // *Crystals* **7** (2017) 315.
[25] H. Conrad // *Metall. Mater. Trans. A* **35** (2004) 2681.
[26] H. Conrad // *Mater. Sci. Eng. A* **341** (2003) 216.
[27] M. Kato // *Mater. Sci. Eng. A* **516** (2009) 276.
[28] I.A. Ovid'ko and A.G. Sheinerman // *Rev. Adv. Mater. Sci.* **50** (2017) 37.
[29] J.P. Hirth and J. Lothe, *Theory of Dislocations* (Wiley, New York, 1982).
[30] R.W. Armstrong // *Mater. Trans.* **55** (2014) 2.
[31] R.P. Carreker and W.R. Hibbard // *Acta Metall.* **1** (1953) 657.
[32] Y.M. Wang and E. Ma // *Appl. Phys. Lett.* **83** (2003) 3165.
[33] Q. Wei, S. Cheng, K.T. Ramesh and E. Ma // *Mater. Sci. Eng. A* **381** (2004) 71.
[34] L. Lu, S.X. Li and K. Lu // *Scripta Mater.* **45** (2001) 1163.
[35] H. Van Swygenhoven, M. Spaczer and A. Caro // *Acta Mater.* **47** (1999) 3117.
[36] M. Zehetbauer and V. Seumer // *Acta Metall. Mater.* **41** (1993) 577.
[37] J. Friedel, *Dislocations* (Pergamon Press, Oxford, 1964).
[38] S.V. Divinski, G. Reglitz and G. Wilde // *Acta Mater.* **58** (2010) 386.
[39] R.A. Masumura, P.M. Hazzledine and C.S. Pande // *Acta Mater.* **46** (1998) 4527.
[40] A.A. Fedorov, M.Y. Gutkin and I.A. Ovid'ko // *Scripta Mater.* **47** (2002) 51.